Journal of Biosciences and Medicines, 2025, 13(12), 247-266
https://www.scirp.org/journal/jbm
ISSN Online: 2327-509X
ISSN Print: 2327-5081

Exploring the Molecular Mechanisms of Yinqiao Shihu Decoction in the Treatment of Hepatocellular Carcinoma Based on Network Pharmacology, Molecular Docking, and Single-Cell Sequencing Analysis

Yazhou Yang[1,2], Yongle Li[2], Xuanhua Chen[3], Xinling Shang[2], Jun Tang[1*], Lihe Jiang[2*]

[1]Department of Gastrointestinal Surgery, The Affiliated Hospital of Youjiang Medical University for Nationalities, Baise, China
[2]School of Clinical Medicine, Youjiang Medical University for Nationalities, Baise, China
[3]Department of Pharmacy, Baise People's Hospital, Baise, China
Email: *tangj202508@163.com, *jianglihe@ymun.edu.cn

How to cite this paper: Yang, Y.Z., Li, Y.L., Chen, X.H., Shang, X.L., Tang, J. and Jiang, L.H. (2025) Exploring the Molecular Mechanisms of Yinqiao Shihu Decoction in the Treatment of Hepatocellular Carcinoma Based on Network Pharmacology, Molecular Docking, and Single-Cell Sequencing Analysis. *Journal of Biosciences and Medicines*, **13**, 247-266.
https://doi.org/10.4236/jbm.2025.1312019

Received: October 26, 2025
Accepted: December 13, 2025
Published: December 16, 2025

Abstract

Objective: To explore the potential molecular mechanisms of Yinqiao Shihu Decoction (YSD) in the treatment of Hepatocellular Carcinoma (HCC) using a network pharmacology-based approach. **Methods:** The chemical constituents of each herb in YSD were retrieved from the TCMSP and TCMID databases, and the active compounds and their corresponding targets were identified. Differentially expressed genes were obtained from the GEO and TCGA databases, while key disease-related targets were screened using the TTD, OMIM, and GeneCards databases. Protein-protein interaction networks were constructed, followed by Gene Ontology enrichment and Kyoto Encyclopedia of Genes and Genomes pathway analyses. Molecular docking between core active components and hub target proteins was performed using AutoDock software. The correlation between the expression of core genes and overall survival in HCC patients was analyzed via the GEPIA2 online platform. Single-cell transcriptomic data (GSE290925) were analyzed using Seurat to explore the cellular distribution of hub genes. **Results:** A total of 161 active compounds and 101 key therapeutic targets of YSD for HCC were identified. ALB, IL6, CASP3, EGFR, and VEGFA were recognized as key hub proteins. Enrichment analysis indicated significant involvement in transcriptional regulation, apoptosis, and PI3K-Akt and MAPK signaling pathways. Quercetin, kaempferol, luteolin, wogonin, and β-sitosterol were identified as major active components, showing strong binding affinities with RAF1, PTGS1, and NCOA2. PTGS1 and

RELA expression were negatively correlated with overall survival in HCC patients. Single-cell analysis revealed that NCOA2, RELA, and RAF1 were highly expressed in monocytes, PTGS1 in NK cells, and CCND1 in fibroblasts, highlighting their potential roles in the HCC microenvironment. **Conclusion:** YSD may treat HCC through a multi-component and multi-target mechanism. Core compounds such as quercetin, kaempferol, luteolin, wogonin, and β-sitosterol act on key targets including ALB, IL6, CASP3, VEGFA, and RAF1 via PI3K-Akt and MAPK pathways. Single-cell analysis indicated cell-type-specific expression of hub genes, suggesting that YSD may regulate tumor immunity and microenvironment. These findings provide a theoretical basis for YSD's clinical application in HCC.

Keywords

Yinqiao Shihu Decoction, Hepatocellular Carcinoma, Network Pharmacology, Key Targets

1. Introduction

Hepatocellular Carcinoma (HCC), the major pathological type of primary liver cancer, originates from hepatic epithelial cells and accounts for approximately 75-85% of primary liver cancers in Asia [1]. It is one of the most common malignant tumors of the liver. According to global cancer statistics, there were 18.1 million new cancer cases and 9.6 million cancer-related deaths worldwide in 2018, with approximately 782,000 deaths attributed to liver cancer [2]. China bears a disproportionately high burden of this disease.

Yinqiao is a traditional Chinese medicine formula primarily composed of *Lonicera japonica* (Yin Hua) and *Forsythia suspensa* (Lian Qiao), which are known for their heat-clearing and detoxifying effects. It is commonly used for the treatment of wind-heat type common cold and upper respiratory tract infections [3] [4]. Building on the Yinqiao formula, researchers have combined it with Liuwei Dihuang Wan and added *Dendrobium officinale* (Shi Hu) to develop Yinqiao Shihu Decoction, a compound formula that integrates the therapeutic principles of nourishing Yin, tonifying the kidneys, and clearing heat and detoxifying. Clinical practice has demonstrated that YSD is effective in alleviating symptoms associated with chronic urinary tract infections and kidney Yin deficiency, and it has also shown potential benefits in adjuvant treatment for chronic glomerulonephritis, postoperative recovery after renal carcinoma, and systemic lupus erythematosu.

However, research on YSD remains limited, and its potential role in tumor therapy, particularly in liver cancer, has yet to be fully elucidated. Research on Traditional Chinese Medicine (TCM) and compound formulas often faces challenges such as low detection sensitivity and insufficiently reliable evaluation indices, which hinder the systematic and comprehensive elucidation of their molecular mechanisms.

Therefore, this study employed network pharmacology to explore the potential mechanisms of YSD in the treatment of HCC, providing a theoretical foundation for subsequent experimental design and optimization.

2. Methods

2.1. Composition of Yinqiao Shihu Decoction (YSD)

Yinqiao Shihu Decoction (YSD) is derived from the Yinqiao Formula, Liuwei Dihuang Pill, and *Dendrobium officinale*, as documented in The Clinical Handbook of Chinese Prescriptions and previous literature. The decoction consists of nine herbal ingredients: *Rehmannia glutinosa* (Shudihuang), *Cornus officinalis* (Shanzhuyu), *Dioscorea opposita* (Shanyao), *Poria cocos* (Fuling), *Alisma orientale* (Zexie), *Paeonia suffruticosa* Andrews (Mudanpi), *Lonicera japonica* (Jinyinhua), *Forsythia suspensa* (Lianqiao), and *Dendrobium nobile* (Shihu).

2.2. Screening of Active Ingredients and Target Collection of Yinqiao Shihu Decoction

The Traditional Chinese Medicine Systems Pharmacology Database (TCMSP) was used to retrieve the chemical constituents of each herb in the formula by searching the keywords "*Lonicera japonica*" (Jinyinhua), "*Rehmannia glutinosa*" (Shudihuang), "*Paeonia suffruticosa*" (Mudanpi), "*Cornus officinalis*" (Shanzhuyu), "*Alisma orientale*" (Zexie), "*Poria cocos*" (Fuling), "*Dioscorea opposita*" (Shanyao), and "*Forsythia suspensa*" (Lianqiao). The active components were screened based on pharmacokinetic parameters of Absorption, Distribution, Metabolism, and Excretion (ADME), with Oral Bioavailability (OB) and Drug-Likeness (DL) serving as key indicators. The constituents of Dendrobium (Shihu) were retrieved from the Traditional Chinese Medicine Integrated Database (TCMID) and cross-validated with the TCMSP database to identify bioactive compounds. The chemical structures of these active ingredients were obtained from the databases and redrawn using ChemDraw Ultra 8.0. The corresponding two-dimensional (2D) structures were converted into three-dimensional (3D) conformations using Chem3D Ultra 8.0 and saved in mol2 format. Potential targets of the active compounds were collected from the TCMSP database. Protein names were standardized and converted into corresponding gene names using Perl scripts and the UniProt database.

2.3. Identification of HCC-Related Targets

The GSE62232 dataset, containing data from 10 normal liver tissue samples and 81 Hepatocellular Carcinoma (HCC) tissue samples, was obtained from the Gene Expression Omnibus (GEO) database. Meanwhile, the TCGA-LIHC dataset, including 50 normal liver tissue samples and 374 primary HCC tissue samples, was downloaded from The Cancer Genome Atlas (TCGA) database. Differential expression analyses were conducted on both datasets using the GEO2R web tool and R packages, and the overlapping Differentially Expressed Genes (DEGs) were

identified based on the results. To further determine HCC-related targets, the Therapeutic Target Database (TTD), Online Mendelian Inheritance in Man (OMIM), and GeneCards databases were queried using the keyword "Hepatocellular Carcinoma", and the identified targets were considered as candidate genes. The DEGs and candidate targets were then integrated using the Venny 2.1.0 online tool and intersected with the targets of YSD. The overlapping genes, visualized in a Venn diagram, were identified as the potential key targets of YSD in the treatment of HCC.

2.4. Construction of the Protein-Protein Interaction (PPI) Network

To evaluate the potential protein-protein interactions among the identified key targets, these targets were imported into the database for analysis. The resulting interaction data were saved as a TSV file and subsequently imported into Cytoscape software to construct the protein-protein interaction network. The top five core target proteins were then identified based on their degree of connectivity within the network.

2.5. GO and KEGG Enrichment Analysis of Core Targets

Biological pathways perform specific physiological functions through the interactions among their constituent target proteins, providing the mechanistic basis for understanding the clinical manifestations of diseases [5]. The core target genes were imported into the DAVID database, and official gene symbols were used for identification. Gene Ontology (GO) functional enrichment analysis and Kyoto Encyclopedia of Genes and Genomes (KEGG) pathway enrichment analysis were then conducted, and the top 15 significantly enriched results were selected for visualization.

2.6. Construction of the "Active Compound-Key Target-Pathway" Network

Based on the KEGG enrichment analysis results, an "Active Compound-Key Target-Pathway" network was constructed using Cytoscape 3.7.2, reflecting the interactions between active compounds and key targets as well as between key targets and pathways. In this network, nodes represent active compounds, targets, and pathways, while edges indicate the interactions among them. The merge function was used to integrate this network with the Protein-Protein Interaction (PPI) network, and topological analysis was performed using the Network Analyzer plugin. Higher degree values indicate greater importance of the target in the therapeutic process of YSD against HCC. Based on the degree values, the top five core target proteins and corresponding core active compounds were identified.

2.7. Molecular Docking

The selected core target proteins were used as receptors, and their corresponding crystal structures were obtained from the Protein Data Bank (PDB). The active

compounds of YSD-quercetin, kaempferol, luteolin, wogonin, and β-sitosterol-were employed as ligands, with the previously saved mol2 files uploaded. Molecular docking of the core target proteins and ligands was performed using AutoDockTools 1.5.6. Grid energy calculations were conducted using AutoGrid, and the Genetic Algorithm was applied for docking. Binding energy was used to assess the affinity between the receptor and ligand.

2.8. Prognostic and Single-Cell Analysis of Key Candidate Genes

To further elucidate the potential key genes linking YSD and Hepatocellular Carcinoma (HCC) progression, results from multiple analytical layers were integrated. Genes that were simultaneously ranked among the top nodes in the PPI network and included in the "Active Compound-Key Target-Pathway" network were first shortlisted. Among these, those exhibiting strong binding affinities to major active compounds (binding energy < −5.0 kcal/mol) in molecular docking and previously reported to be associated with tumorigenesis or HCC development were prioritized. Based on these criteria, five representative genes—NCOA2, PTGS1, RELA, CCND1, and RAF1—were selected for subsequent prognostic and single-cell analyses.

The prognostic significance of these targets was evaluated using the GEPIA2 online platform. A 95% confidence interval was applied, and the median expression level (50%) was used as the cut-off value to classify patients into high- and low-expression groups. The correlations between the expression levels of NCOA2, PTGS1, RELA, CCND1, and RAF1 and Overall Survival (OS) outcomes in HCC patients were then analyzed.

2.9. Single-Cell RNA Sequencing Analysis

We analysed three single-cell RNA sequencing (scRNA-seq) samples from the GEO database (GSM8825750, GSM8825751, GSM8825752) belonging to the series GSE290925 ("Single-Cell Transcriptomic Profiling of the Tumor Microenvironment in Treatment-Naive Hepatocellular Carcinoma Patients"). Each sample represents a surgical puncture tumour specimen obtained before any treatment from a Hepatocellular Carcinoma (HCC) patient. The scRNA libraries were constructed using the 10× Genomics Chromium Single Cell 3' Reagent v3 Kit and sequenced on an Illumina NextSeq 500 platform according to the manufacturer's protocol. Cells with mitochondrial gene content exceeding 25% were filtered out, followed by data normalization using the LogNormalize method, and 2000 highly variable genes were selected. The Harmony algorithm was subsequently applied to correct batch effects. Cell clustering was performed based on Principal Component Analysis (PCA) and t-distributed Stochastic Neighbor Embedding (t-SNE). Cell type annotation was conducted using the SingleR package in conjunction with a human primary cell atlas, and the expression patterns of core genes were visualized on t-SNE plots, providing a systematic characterization of single-cell heterogeneity.

3. Result

3.1. Screening of Active Compounds and Target Collection of Yinqiao Shihu Decoction

Through database retrieval and screening, 2 compounds of *Rehmannia glutinosa* (Shudihuang), 20 compounds of *Cornus officinalis* (Shanzhuyu), 16 compounds of *Dioscorea opposita* (Shanyao), 10 compounds of *Alisma orientale* (Zexie), 11 compounds of *Paeonia suffruticosa* (Mudanpi), 15 compounds of *Poria cocos* (Fuling), 23 compounds of *Lonicera japonica* (Jinyinhua), 23 compounds of *Forsythia suspensa* (Lianqiao), and 3 compounds of *Dendrobium* (Shihu) were identified (two additional Dendrobium compounds with drug-likeness < 0.18 were included due to limited matches across the two databases; see **Appendix** Table A1). Targets of these active compounds were collected from the TCMSP database and mapped to gene symbols using the UniProt database. After removing duplicates, a total of 120 unique targets were obtained.

3.2. Identification of HCC-Related Targets

Differential expression analysis was performed using sample data from the GEO and TCGA databases, combined with searches in the TTD, OMIM, and GeneCards databases. A total of 949 overlapping differentially expressed genes and 7100 disease-related targets were identified. In the TCGA dataset, 7821 genes were upregulated and 1493 were downregulated (Figure 1(A)). Based on the intersection with the targets of YSD, 101 key targets for HCC treatment were obtained (Figure 1(B), Figure 1(C)).

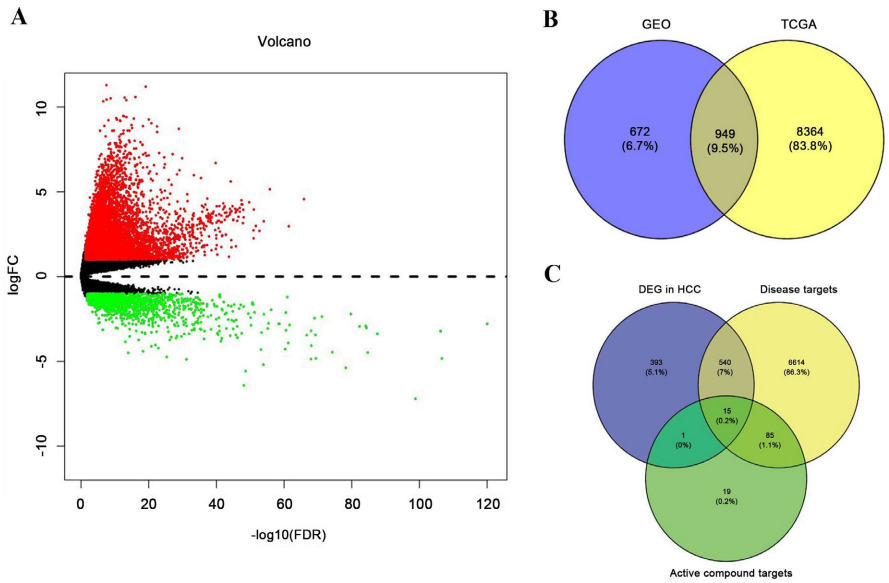

Figure 1. Screening of active compounds and identification of key targets related to Hepatocellular Carcinoma (HCC). (A) Differentially expressed genes in HCC vs. normal tissues from TCGA, including 7821 upregulated and 1493 downregulated genes. (B) (C) Venn diagram showing overlap between YSD targets and HCC-related genes; 101 intersecting genes were identified as key targets.

3.3. Construction of the Protein-Protein Interaction Network

The identified key targets were input into the STRING database to obtain the Protein-Protein Interaction (PPI) network, and the resulting interaction data were imported into Cytoscape for network construction (see **Appendix** Figure A1(A)). In the network, larger nodes indicate higher degree values. ALB, IL6, CASP3, EGFR, and VEGFA exhibited the highest degrees and were identified as the core target proteins.

3.4. GO Functional Annotation and KEGG Pathway Enrichment

GO functional enrichment analysis using the DAVID online database identified a total of 121 GO terms, including 79 Biological Process (BP) terms, 18 Cellular Component (CC) terms, and 24 Molecular Function (MF) terms. KEGG pathway enrichment analysis revealed 75 significantly enriched pathways. The major biological processes involved positive/negative regulation of RNA polymerase II promoter transcription, DNA transcription, negative regulation of apoptosis, and negative regulation of cell proliferation. Cellular components were primarily associated with the nucleus, cytoplasm, extracellular exosome, and cytosol. Molecular functions included transcription factor activity, sequence-specific DNA binding, zinc ion binding, and transcription activator activity. Significantly enriched pathways included PI3K-Akt, TNF, MAPK, cancer-related pathways, and hepatitis B signaling (see **Appendix** Figures A1(B)-(E)).

3.5. Construction and Analysis of the "Active Compound-Key Target-Pathway" Network

The constructed "Active Compound-Key Target-Pathway" network comprised 62 active compounds, 101 target proteins, and 20 pathways. In the network, red nodes represent active compounds, blue nodes represent key targets, and green nodes represent pathways (see **Appendix** Figure A2(A)). Based on node degree, the top five core targets were identified as MYC, ESR1, CCND1, ALB, and AR (in addition to the core targets identified from the PPI network), while the top five core active compounds were quercetin, kaempferol, luteolin, wogonin, and β-sitosterol, which were selected for subsequent analyses.

3.6. Molecular Docking and Analysis

The crystal structures of the 10 selected core targets were downloaded from the Protein Data Bank (PDB), and molecular docking was performed between the core targets and core active compounds (see **Appendix** Figure A1(B)). The results indicated that the five selected core active compounds exhibited low binding energies with most core targets, with β-sitosterol and wogonin showing the strongest binding affinities. Targets including RAF1, PTGS1, and NCOA2 demonstrated favorable binding with the core compounds; these proteins have been previously reported in HCC-related studies, and their molecular docking results showed relatively low binding energies (see **Appendix** Figures A1(C)-(F)).

3.7. Prognostic Analysis of Key Targets NCOA2, PTGS1, RELA, CCND1, and RAF1

Analysis revealed that the mRNA expression levels of PTGS1 and RELA were significantly associated with Overall Survival (OS) in patients ($P < 0.05$), indicating that both serve as adverse prognostic factors in HCC (Figure 2).

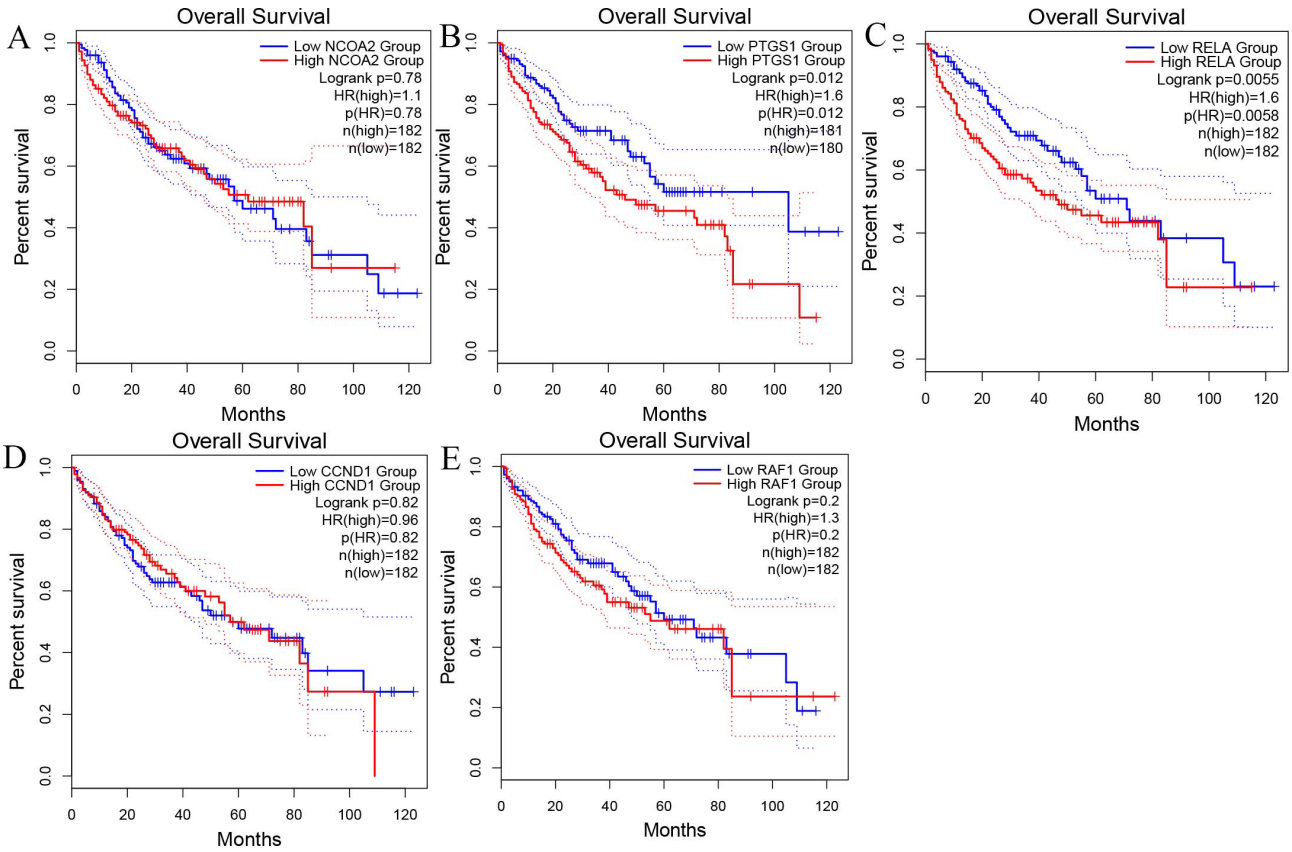

Figure 2. Survival analysis of RAF1 and EGFR in HCC patients.

3.8. Single-Cell Data Quality Control and Batch Correction

Cells with mitochondrial gene content exceeding 25% were filtered out from the single-cell dataset (Figure 3(A)). After filtering, the number of detected RNAs was highly positively correlated with the number of detected molecules ($R = 0.91$) (Figure 3(B)). Batch effects were subsequently corrected using the Harmony package, and t-SNE plots were generated before and after batch correction (Figure 3(C), Figure 3(D)). The first 10 Principal Components (PCs) were selected for clustering analysis (Figure 3(E)).

3.9. Expression Patterns of Key Genes NCOA2, PTGS1, RELA, CCND1, and RAF1 at the Single-Cell Level

Cell type annotation was performed using the SingleR package, classifying the cell populations into T cells, monocytes, macrophages, fibroblasts, tissue stem cells, and NK cells (Figure 4(A)). The results demonstrated that NCOA2, RELA, and

RAF1 exhibited the highest average expression levels in monocytes, PTGS1 showed the highest expression in NK cells, and CCND1 displayed the highest expression in fibroblasts (Figure 4(B)).

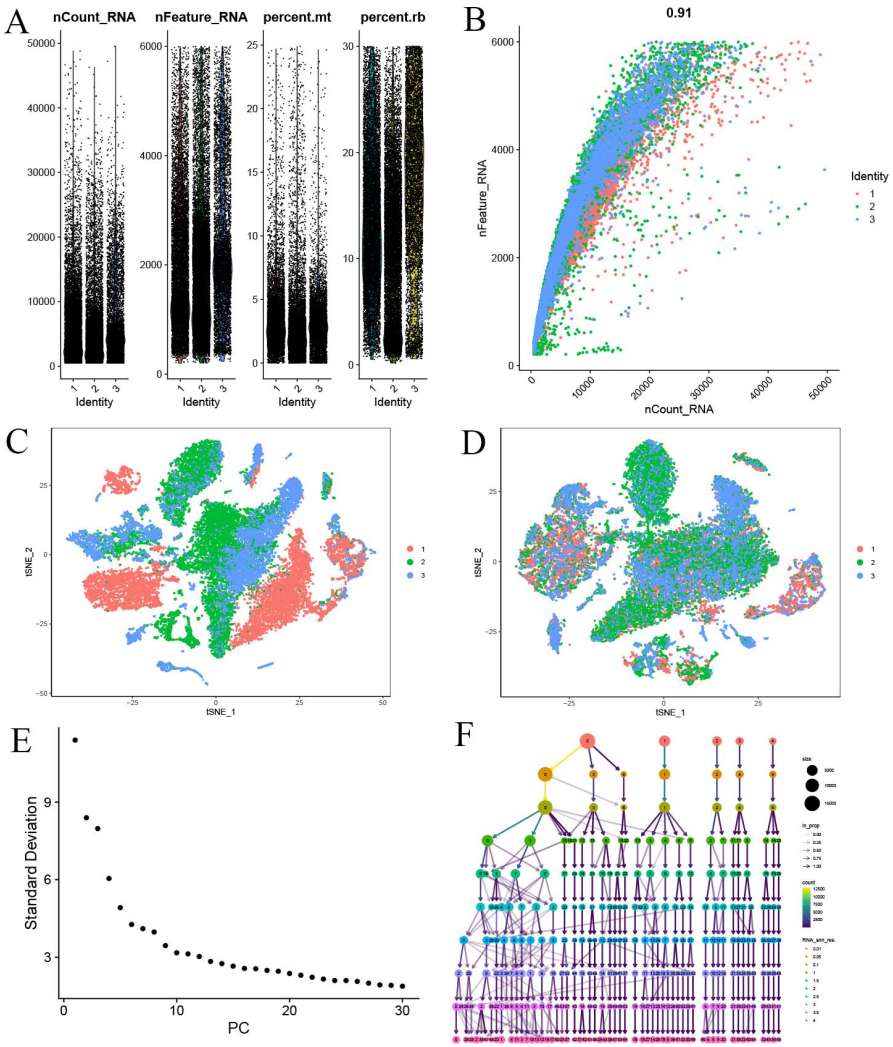

Figure 3. Quality control and batch correction of single-cell data. (A) Cells with >25% mitochondrial gene content were removed. (B) A strong positive correlation was observed between the number of detected genes and UMIs (R = 0.91). (C) (D) t-SNE visualization before and after batch correction using Harmony. (E) The top 10 Principal Components (PCs) were selected based on variance. (F) Clustering was performed at a resolution of 1 for downstream analyses.

4. Discussion

Yinqiao Shihu Decoction (YSD) originates from a modern formula, and there are few clinical or pharmacological studies available regarding its therapeutic effects, particularly against Hepatocellular Carcinoma (HCC). Therefore, this study aimed to explore the potential mechanisms by which YSD exerts its anti-HCC effects using an integrated approach combining network pharmacology, molecular docking, and single-cell transcriptomic analysis.

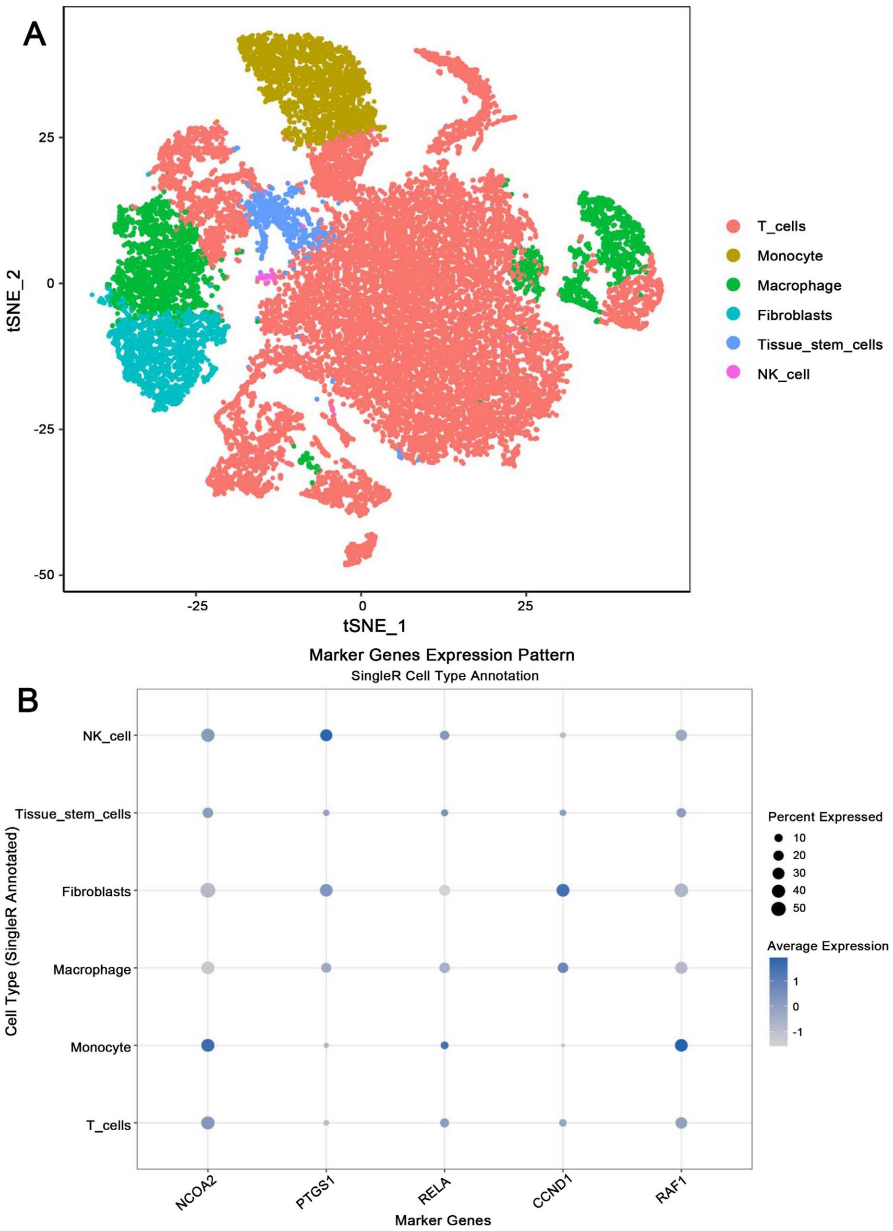

Figure 4. Cell type annotation and expression profiles of core genes. (A) Cell populations were annotated using the SingleR package. (B) NCOA2, RELA, and RAF1 were highly expressed in monocytes, PTGS1 in NK cells, and CCND1 in fibroblasts.

In this study, we first identified the active compounds and their corresponding targets of YSD from multiple databases and intersected them with HCC-related genes to obtain potential therapeutic targets. Protein-protein interaction (PPI) network analysis revealed that ALB, IL6, CASP3, EGFR, and VEGFA had high connectivity and interacted with multiple other targets, suggesting that they might play pivotal roles in the anti-HCC effects of YSD. GO and KEGG enrichment analyses further indicated that these targets were mainly enriched in PI3K-Akt, TNF, and MAPK signaling pathways. In the constructed "active compound-key target-pathway" network, quercetin, kaempferol, luteolin, wogonin, and β-sitos-

terol exhibited high degree values, suggesting that they are the major bioactive components of the decoction. Moreover, NCOA2, PTGS1, RELA, CCND1, and RAF1 were identified as hub genes in the network. Molecular docking analysis confirmed that these core compounds had favorable binding affinities with the corresponding key proteins. Molecular docking analysis further confirmed that these five core active compounds exhibited strong binding affinities with most hub targets, with β-sitosterol and wogonin showing the lowest binding energies. Among them, RAF1, PTGS1, and NCOA2 displayed particularly favorable binding interactions. These results suggest that YSD may exert therapeutic effects against HCC through multi-component, multi-target, and multi-pathway interactions.

Survival analysis revealed that high mRNA expression levels of PTGS1 and RELA were significantly associated with poorer overall survival in HCC patients, indicating that they might serve as adverse prognostic factors. Single-cell RNA sequencing analysis further showed that these key genes displayed cell-type-specific expression patterns: NCOA2, RELA, and RAF1 were mainly expressed in monocytes, PTGS1 showed the highest expression in NK cells, and CCND1 was predominantly expressed in fibroblasts. These findings suggest that YSD may regulate multiple cell types in the tumor microenvironment, thereby affecting HCC progression.

Mechanistically, Interleukin-6 (IL-6), a cytokine produced by various cell types, plays a crucial role in immune activation, signal transduction, and inflammation [6]. The IL-6/STAT3 signaling pathway has been shown to promote HCC cell growth and drug resistance, whereas its inhibition can polarize macrophages toward the M1 phenotype, thereby reducing the proliferation, invasion, and migration of HCC cells while promoting apoptosis. CASP3 is a critical executioner in apoptosis, and its downregulation suppresses apoptosis and promotes tumor growth [7]. The Epidermal Growth Factor Receptor (EGFR) pathway, particularly EGFR-PI3K-PDK1, is also crucial in hepatocarcinogenesis, activating YAP signaling to enhance cell proliferation [8]. VEGFA plays a central role in tumor angiogenesis by promoting endothelial cell proliferation and vascular permeability; inhibition of VEGFA signaling suppresses tumor growth and angiogenesis [9]. RAF1, acting as an oncogene, promotes HCC progression, and its inhibition can effectively halt tumor development [10].

The PI3K/Akt signaling pathway is widely recognized as a key regulator of cell proliferation, invasion, migration, and apoptosis in liver cancer, particularly Hepatocellular Carcinoma (HCC) [11]. Studies have shown that activation of the PI3K/Akt pathway can promote glucose uptake, glycolysis, proliferation, epithelial-mesenchymal transition, expression of matrix metalloproteinases, and angiogenesis in HCC cells, thereby enhancing their invasiveness and metastatic potential, while simultaneously inhibiting apoptosis and autophagy to facilitate tumor cell survival [12] [13]. Our findings indicate that several critical targets of YSD, such as EGFR, GSK3B, MTOR, and VEGFA, are enriched in the PI3K-Akt signal-

ing pathway, implying that the decoction may interfere with HCC cell proliferation, invasion, and migration by modulating this pathway. Additionally, YSD may regulate the TNF signaling pathway through CASP3 and IL6, thereby affecting tumor growth and metastasis. The MAPK signaling pathway, which plays a vital role in cell proliferation, apoptosis, invasion, and angiogenesis, is also significantly involved in HCC pathogenesis; its inhibition can suppress tumor growth and angiogenesis [14]. Collectively, these results suggest that YSD exerts multi-component, multi-target, and multi-pathway synergistic effects to interfere with HCC progression.

However, it should be noted that this study is entirely based on computational predictions. The predicted compound-target interactions and potential therapeutic effects of YSD still require experimental validation in vitro and in vivo to confirm their reliability. Furthermore, these findings provide guidance for future research and clinical translation. Key genes identified, such as PTGS1 and RELA, may serve as potential biomarkers to monitor the efficacy of YSD treatment in HCC, and could be considered as targets for subsequent mechanistic and therapeutic studies.

Building on these insights, this study systematically elucidated the potential mechanisms of YSD in treating hepatocellular carcinoma through an integrated approach combining network pharmacology, molecular docking, and single-cell transcriptomic analysis. The findings indicate that the decoction may act through major active components—quercetin, kaempferol, luteolin, wogonin, and β-sitosterol—to target multiple key genes such as ALB, IL6, CASP3, and VEGFA, thereby modulating signaling pathways including PI3K-Akt, TNF, and MAPK to suppress HCC development. Moreover, high expression levels of PTGS1 and RELA were significantly associated with poor prognosis in HCC patients, suggesting that these genes may serve as important prognostic biomarkers and potential therapeutic targets for YSD in the treatment of HCC.

Funding

Guangxi Natural Science Foundation (Grant No. 2025GXNSFHA069094), Baise City Science and Technology Plan Project (Science and Technology Infrastructure Support Program) (Grant No.ZJ252812), High-Level Talents Introduction Program of Youjiang Medical University for Nationalities (Grant No. YY2021sk02), National Undergraduate Innovation and Entrepreneurship Training Program (Grant No. 202310599005), Guangxi Undergraduate Innovation and Entrepreneurship Training Program (Grant Nos. 202410599001, S202410599049).

Author Contributions

Ya-Zhou Yang: Writing—review & editing, Writing—original draft, Software, Investigation, Formal analysis, Data curation, Conceptualization.

Yong-Le Li: review & editing, Software, Investigation, Formal analysis, Data curation, Conceptualization.

Xuan-Hua Chen: review & editing.

Xin-Ling Shang: review & editing.

Jun Tang: Conceptualization, Supervision, Methodology, Writing—review & editing, Visualization, Software, Resources, Funding acquisition, Formal analysis.

Li-He Jiang: Conceptualization, Supervision, Methodology, Writing—review & editing, Visualization, Software, Resources, Funding acquisition, Formal analysis.

Conflicts of Interest

The authors declare that they have no known competing financial interests or personal relationships that could have appeared to influence the work reported in this paper.

References

[1] Zhang, C.H., Cheng, Y., Zhang, S., Fan, J. and Gao, Q. (2022) Changing Epidemiology of Hepatocellular Carcinoma in Asia. *Liver International*, **42**, 2029-2041. https://doi.org/10.1111/liv.15251

[2] Huang, J., Lok, V., Ngai, C.H., Chu, C., Patel, H.K., Thoguluva Chandraseka, V., *et al.* (2021) Disease Burden, Risk Factors, and Recent Trends of Liver Cancer: A Global Country-Level Analysis. *Liver Cancer*, **10**, 330-345. https://doi.org/10.1159/000515304

[3] Guo, R., Zhao, M., Liu, H., Su, R., Mao, Q., Gong, L., *et al.* (2021) Uncovering the Pharmacological Mechanisms of Xijiao Dihuang Decoction Combined with Yinqiao Powder in Treating Influenza Viral Pneumonia by an Integrative Pharmacology Strategy. *Biomedicine & Pharmacotherapy*, **141**, Article 111676. https://doi.org/10.1016/j.biopha.2021.111676

[4] Sum, C.H., Li, T.W., Zhang, H., Hung, H.Y., Fong, B.Y.F., Lin, W.L., *et al.* (2023) Assessing the Efficacy and Safety of Yinqiao Powder-Maxing Ganshi Decoction in the Treatment of the Major Symptoms of Mild and Moderate COVID-19 by Telemedicine–study Protocol for a Randomized, Double-Blind, Placebo-Controlled Trial. *Frontiers in Pharmacology*, **14**, Article 1261338. https://doi.org/10.3389/fphar.2023.1261338

[5] Liu, J., Pei, M., Zheng, C., Li, Y., Wang, Y., Lu, A., *et al.* (2013) A Systems-Pharmacology Analysis of Herbal Medicines Used in Health Improvement Treatment: Predicting Potential New Drugs and Targets. *Evidence-Based Complementary and Alternative Medicine*, **2013**, 1-17. https://doi.org/10.1155/2013/938764

[6] Tanaka, T. and Kishimoto, T. (2014) The Biology and Medical Implications of Interleukin-6. *Cancer Immunology Research*, **2**, 288-294. https://doi.org/10.1158/2326-6066.cir-14-0022

[7] Zhang, G., Zeng, X., Zhang, R., Liu, J., Zhang, W., Zhao, Y., *et al.* (2016) Dioscin Suppresses Hepatocellular Carcinoma Tumor Growth by Inducing Apoptosis and Regulation of TP53, BAX, BCL2 and Cleaved Casp3. *Phytomedicine*, **23**, 1329-1336. https://doi.org/10.1016/j.phymed.2016.07.003

[8] Xia, H., Dai, X., Yu, H., Zhou, S., Fan, Z., Wei, G., *et al.* (2018) EGFR-PI3K-PDK1 Pathway Regulates YAP Signaling in Hepatocellular Carcinoma: The Mechanism and Its Implications in Targeted Therapy. *Cell Death & Disease*, **9**, Article No. 269. https://doi.org/10.1038/s41419-018-0302-x

[9] Yang, W., Li, Z., Qin, R., Wang, X., An, H., Wang, Y., et *al.* (2019) YY1 Promotes

Endothelial Cell-Dependent Tumor Angiogenesis in Hepatocellular Carcinoma by Transcriptionally Activating Vegfa. *Frontiers in Oncology*, **9**, Article 1187. https://doi.org/10.3389/fonc.2019.01187

[10] Wang, T.H., Hsueh, C., Chen, C., Li, W., Yeh, C., Lian, J., *et al.* (2018) Melatonin Inhibits the Progression of Hepatocellular Carcinoma through MicroRNA Let7i-3p Mediated RAF1 Reduction. *International Journal of Molecular Sciences*, **19**, Article 2687. https://doi.org/10.3390/ijms19092687

[11] Tian, L., Smit, D.J. and Jücker, M. (2023) The Role of PI3K/Akt/mTOR Signaling in Hepatocellular Carcinoma Metabolism. *International Journal of Molecular Sciences*, **24**, Article 2652. https://doi.org/10.3390/ijms24032652

[12] Paskeh, M.D.A., Ghadyani, F., Hashemi, M., Abbaspour, A., Zabolian, A., Javanshir, S., *et al.* (2023) Biological Impact and Therapeutic Perspective of Targeting PI3K/Akt Signaling in Hepatocellular Carcinoma: Promises and Challenges. *Pharmacological Research*, **187**, Article 106553. https://doi.org/10.1016/j.phrs.2022.106553

[13] Wu, Y., Zhang, Y., Qin, X., Geng, H., Zuo, D. and Zhao, Q. (2020) PI3K/Akt/mTOR Pathway-Related Long Non-Coding RNAs: Roles and Mechanisms in Hepatocellular Carcinoma. *Pharmacological Research*, **160**, Article 105195. https://doi.org/10.1016/j.phrs.2020.105195

[14] Asl, E.R., Amini, M., Najafi, S., Mansoori, B., Mokhtarzadeh, A., Mohammadi, A., *et al.* (2021) Interplay between MAPK/ERK Signaling Pathway and MicroRNAs: A Crucial Mechanism Regulating Cancer Cell Metabolism and Tumor Progression. *Life Sciences*, **278**, Article 119499. https://doi.org/10.1016/j.lfs.2021.119499

Appendix

Table A1. Information on the active compounds of Yinqiao Shihu Decoction.

Mol ID	Active compound	OB (%)	DL	Single herb
MOLO00359	Sitosterol	36.91	0.75	*Rehmannia glutinosa* (Shu Dihuang)
MOLO00449	Stigmasterol	43.83	0.76	*Rehmannia glutinosa* (Shu Dihuang)
MOLO01494	Mandenol	42	0.19	*Cornus officinalis* (Shanzhuyu)
MOLO01495	Ethyl linolenate	46.1	0.2	*Cornus officinalis* (Shanzhuyu)
MOLO01771	Poriferast-5-en-3beta-ol	36.91	0.75	*Cornus officinalis* (Shanzhuyu)
MOL002879	Diop	43.59	0.39	*Cornus officinalis* (Shanzhuyu)
MOLO02883	Ethyl oleate (NF)	32.4	0.19	*Cornus officinalis* (Shanzhuyu)
MOLO03137	Leucanthoside	32.12	0.78	*Cornus officinalis* (Shanzhuyu)
MOLO00358	Beta-sitosterol	36.91	0.75	*Cornus officinalis* (Shanzhuyu)
MOL000359	Sitosterol	36.91	0.75	*Cornus officinalis* (Shanzhuyu)
MOLO00449	Stigmasterol	43.83	0.76	*Cornus officinalis* (Shanzhuyu)
MOLO05360	Malkangunin	57.71	0.63	*Cornus officinalis* (Shanzhuyu)
MOL005481	2,6,10,14,18-pentamethylicosa-2,6,10,14,18-pentaene	33.4	0.24	*Cornus officinalis* (Shanzhuyu)
MOLO05486	3,4-Dehydrolycopen-16-al	46.64	0.49	*Cornus officinalis* (Shanzhuyu)
MOLO05489	3,6-Digalloylglucose	31.42	0.66	*Cornus officinalis* (Shanzhuyu)
MOLO05503	Cornudentanone	39.66	0.33	*Cornus officinalis* (Shanzhuyu)
MOLO05530	Hydroxygenkwanin	36.47	0.27	*Cornus officinalis* (Shanzhuyu)
MOLO05531	Telocinobufagin	69.99	0.79	*Cornus officinalis* (Shanzhuyu)
MOLO08457	Tetrahydroalstonine	32.42	0.81	*Cornus officinalis* (Shanzhuyu)
MOLOO0554	Gallic acid-3-0-(6'-0-galloyl)-glucoside	30.25	0.67	*Cornus officinalis* (Shanzhuyu)
MOLO05552	gemin D	68.83	0.56	*Cornus officinalis* (Shanzhuyu)
MOLO05557	Lanosta-8,24-dien-3-ol,3-acetate	44.3	0.82	*Cornus officinalis* (Shanzhuyu)
MOLO01559	Piperlonguminine	30.71	0.18	*Dioscorea opposita* (Shanyao)
MOL001736	(-)-taxifolin	60.51	0.27	*Dioscorea opposita* (Shanyao)
MOLO00310	Denudatin B	61.47	0.38	*Dioscorea opposita* (Shanyao)
MOLO00322	Kadsurenone	54.72	0.38	*Dioscorea opposita* (Shanyao)
MOL005429	Hancinol	64.01	0.37	*Dioscorea opposita* (Shanyao)
MOLO05430	Hancinone C	59.05	0.39	*Dioscorea opposita* (Shanyao)
MOL005435	24-Methylcholest-5-enyl-3belta-0-glucopyranoside_qt	37.58	0.72	*Dioscorea opposita* (Shanyao)
MOLO05438	Campesterol	37.58	0.71	*Dioscorea opposita* (Shanyao)
MOLO05440	Isofucosterol	43.78	0.76	*Dioscorea opposita* (Shanyao)
MOLO00449	Stigmasterol	43.83	0.76	*Dioscorea opposita* (Shanyao)
MOL005458	DioscoresideC_qt	36.38	0.87	*Dioscorea opposita* (Shanyao)
MOLO00546	Diosgenin	80.88	0.81	*Dioscorea opposita* (Shanyao)
MOLO05461	Doradexanthin	38.16	0.54	*Dioscorea opposita* (Shanyao)

Continued

MOLO05463	Methylcimicifugoside_qt	31.69	0.24	*Dioscorea opposita* (Shanyao)
MOLO05465	AIDS180907	45.33	0.77	*Dioscorea opposita* (Shanyao)
MOL000953	CLR	37.87	0.68	*Dioscorea opposita* (Shanyao)
MOLO00359	Sitosterol	36.91	0.75	*Alisma orientale* (Zexie)
MOLO00830	Aliso1 B	34.47	0.82	*Alisma orientale* (Zexie)
MOL000831	Alisol B monoacetate	35.58	0.81	*Alisma orientale* (Zexie)
MOLO00832	Alisol, b,23-acetate	32.52	0.82	*Alisma orientale* (Zexie)
MOL000849	16β-methoxyalisol B monoacetate	32.43	0.77	*Alisma orientale* (Zexie)
MOL000853	Alisol B	36.76	0.82	*Alisma orientale* (Zexie)
MOLO00854	Alisol C	32.7	0.82	*Alisma orientale* (Zexie)
MOLO00856	Alisol C monoacetate	33.06	0.83	*Alisma orientale* (Zexie)
MOLO02464	1-Monolinolein [(1S,3R)-1-[(2R)-3,3-dimethyloxiran-2-yl]-3-[(5R,8S,9S, 10S,11S,14R)-11	37.18	0.3	*Alisma orientale* (Zexie)
MOL000862	-Hydroxy-4, 4,8, 10, 14-pentamethy1-3-oxo-1,2,5, 6, 7,9,11,12,15,16-decahyd rocyclopenta[a]phenanthren-17-y1]bu tyl] acetate	35.58	0.81	*Alisma orientale* (Zexie)
MOL001925	paeoniflorin_qt	68.18	0.4	*Paeonia suffruticosa* Andrews (Mudanpi)
MOLO00211	Mairin	55.38	0.78	*Paeonia suffruticosa* Andrews (Mudanpi)
MOLO00359	Sitosterol	36.91	0.75	*Paeonia suffruticosa* Andrews (Mudanpi)
MOLO00422	Kaempferol	41.88	0.24	*Paeonia suffruticosa* Andrews (Mudanpi)
MOL000492	(+)-catechin	54.83	0.24	*Paeonia suffruticosa* Andrews (Mudanpi)
MOLO07003	Benzoyl paeoniflorin	31.14	0.54	*Paeonia suffruticosa* Andrews (Mudanpi)
MOLO07369	4-0-methylpaeoniflorin_qt	67.24	0.43	*Paeonia suffruticosa* Andrews (Mudanpi)
MOLO07374	5-[[5-(4-methoxyphenyl)-2-furyl] met hylene] barbituric acid	43.44	0.3	*Paeonia suffruticosa* Andrews (Mudanpi)
MOLO07382	Mudanpioside-h_qt 2	42.36	0.37	*Paeonia suffruticosa* Andrews (Mudanpi)
MOLO07384	Paeonidanin_qt	65.31	0.35	*Paeonia suffruticosa* Andrews (Mudanpi)
MOL000098	Quercetin (2R)-2-[(3S,5R.10S.13R.14R,16R.17R) -3,16-dihydroxy-4,4,10,13, 14-pentam	46.43	0.28	*Paeonia suffruticosa* Andrews (Mudanpi)
MOLO00273	Ethyl-2,3, 5, 6, 12, 15, 16, 17-octahydro-1H-cyclopenta[a]phenanthren-17-y1]-6-methylhept-5-enoic acid	30.93	0.81	*Poria cocos* (Fuling)
MOLO00275	Trametenolic acid	38.71	0.8	*Poria cocos* (Fuling)
MOLO00276	7,9(11)-dehydropachymic acid	35.11	0.81	*Poria cocos* (Fuling)
MOL000279	Cerevisterol (2R)-2-[(3S,5R,10S,13R,14R,16R,17R)-3,16-dihydroxy-4,4,10,13, 14-pentam	37.96	0.77	*Poria cocos* (Fuling)
MOL000280	Ethyl-2,3,5, 6, 12,15, 16, 17-octahydro-1H-cyclopenta[a]phenanthren-17-y1]-5-isopropyl-hex-5-enoic acid	31.07	0.82	*Poria cocos* (Fuling)

Continued

MOL000282	Ergosta-7,22E-dien-3beta-ol	43.51	0.72	*Poria cocos* (Fuling)
MOL000283	Ergosterol peroxide (2R)-2-[(5R,10S,13R,14R,16R,17R)-16-hydroxy-3-keto-4,4, 10,13, 14-pentam	40.36	0.81	*Poria cocos* (Fuling)
MOLO00285	Ethy1-1,2,5, 6, 12, 15, 16, 17-oc tahydro cyclopenta[a]phenanthren-17-yl]-5-i sopropyl-hex-5-enoic acid	38.26	0.82	*Poria cocos* (Fuling)
MOL000287	3beta-Hydroxy-24-methylene-8-lanost ene-21-oic acid	38.7	0.81	*Poria cocos* (Fuling)
MOLO00289	Pachymic acid	33.63	0.81	*Poria cocos* (Fuling)
MOLO00290	Poricoic acid A	30.61	0.76	*Poria cocos* (Fuling)
MOLO00291	Poricoic acid B	30.52	0.75	*Poria cocos* (Fuling)
MOLO00292	Poricoic acid C	38.15	0.75	*Poria cocos* (Fuling)
MOLO00296	Hederagenin	36.91	0.75	*Poria cocos* (Fuling)
MOLO00300	Dehydroeburicoic acid	44.17	0.83	*Poria cocos* (Fuling)
MOLO01494	Mandenol	42	0.19	*Lonicera japonica* (Jinyinhua)
MOLO01495	Ethyl linolenate	46.1	0.2	*Lonicera japonica* (Jinyinhua)
MOLO02707	Phytofluene	43.18	0.5	*Lonicera japonica* (Jinyinhua)
MOLO02914	Eriodyctiol (flavanone) (-)-(3R,8S,9R,9aS,10aS)-9-etheny1-8 -(beta-D-glucopyranosyloxy)-2,3,9,9	41.35	0.24	*Lonicera japonica* (Jinyinhua)
MOLO03006	a,10,10a-hexahydro-5-oxo-5H,8H-pyra no[4,3-d] oxazolo[3,2-a] pyridine-3-c arboxylic acid_qt	87.47	0.23	*Lonicera japonica* (Jinyinhua)
MOLO03014	secologanic dibutylacetal_qt	53.65	0.29	*Lonicera japonica* (Jinyinhua)
MOL002773	Beta-carotene	37.18	0.58	*Lonicera japonica* (Jinyinhua)
MOLO03036	ZINC03978781	43.83	0.76	*Lonicera japonica* (Jinyinhua)
MOLO03044	Chryseriol	35.85	0.27	*Lonicera japonica* (Jinyinhua)
MOLO03059	kryptoxanthin	47.25	0.57	*Lonicera japonica* (Jinyinhua)
MOL003062	4,5'-Retro-. beta., beta.-Carotene-3,3'-dione,4',5'-didehydro-	31.22	0.55	*Lonicera japonica* (Jinyinhua)
MOL003095	5-hydroxy-7-methoxy-2-(3,4, hoxyphenyl) chromone	51.96	0.41	*Lonicera japonica* (Jinyinhua)
MOLO03101	7-epi-Vogeloside	46.13	0.58	*Lonicera japonica* (Jinyinhua)
MOLO03108	Caeruloside C	55.64	0.73	*Lonicera japonica* (Jinyinhua)
MOLO03111	Centauroside_qt	55.79	0.5	*Lonicera japonica* (Jinyinhua)
MOLO03117	Ioniceracetalides B_qt	61.19	0.19	*Lonicera japonica* (Jinyinhua)
MOLO03124	XYLOSTOSIDINE	43.17	0.64	*Lonicera japonica* (Jinyinhua)
MOLO03128	dinethylsecologanoside	48.46	0.48	*Lonicera japonica* (Jinyinhua)
MOLO00358	Beta-sitosterol	36.91	0.75	*Lonicera japonica* (Jinyinhua)
MOL000422	Kaempferol	41.88	0.24	*Lonicera japonica* (Jinyinhua)
MOLO00449	Stigmasterol	43.83	0.76	*Lonicera japonica* (Jinyinhua)
MOLO00006	Luteolin	36.16	0.25	*Lonicera japonica* (Jinyinhua)

Continued

MOL000098	Quercetin	46.42	0.28	*Lonicera japonica* (Jinyinhua)
MOLO00173	Wogonin	30.68	0.23	*Forsythia suspensa* (Lianqiao)
MOL003281	20(S)-dammar-24-ene-3 *β*,20-diol-3-acetate (2R,3R,4S)-4-(4-hydroxy-3-methoxy-p	40.23	0.82	*Forsythia suspensa* (Lianqiao)
MOL003283	henyl)-7-methoxy-2,3-dimethylol-tet ralin-6-ol	66.51	0.39	*Forsythia suspensa* (Lianqiao)
MOL003290	(3R,4R)-3,4-bis[(3,4-dimethoxypheny1) methyl] oxolan-2-one	52.3	0.48	*Forsythia suspensa* (Lianqiao)
MOL003295	(+)-pinoresinol monomethyl ether	53.08	0.57	*Forsythia suspensa* (Lianqiao)
MOLO03305	PHILLYRIN	36.4	0.86	*Forsythia suspensa* (Lianqiao)
MOLO03306	ACon1_001697	85.12	0.57	*Forsythia suspensa* (Lianqiao)
MOL003308	(+)-pinoresinol monomethyl ether-4-D-beta-glucoside_qt	61.2	0.57	*Forsythia suspensa* (Lianqiao)
MOL003315	3beta-Acety1-20,25-epoxydammarane-24alpha-ol	33.07	0.79	*Forsythia suspensa* (Lianqiao)
MOLO00211	Mairin	55.38	0.78	*Forsythia suspensa* (Lianqiao)
MOLO03322	FORSYTHINOL	81.25	0.57	*Forsythia suspensa* (Lianqiao)
MOL003330	(-)-Phillygenin	95.04	0.57	*Forsythia suspensa* (Lianqiao)
MOL003344	*β*-amyrin acetate	42.06	0.74	*Forsythia suspensa* (Lianqiao)
MOL003347	Hyperforin	44.03	0.6	*Forsythia suspensa* (Lianqiao)
MOLO03348	Adhyperforin	44.03	0.61	*Forsythia suspensa* (Lianqiao)
MOL003365	Lactucasterol	40.99	0.85	*Forsythia suspensa* (Lianqiao)
MOLO03370	Onjixanthone I	79.16	0.3	*Forsythia suspensa* (Lianqiao)
MOL000358	Beta-sitosterol	36.91	0.75	*Forsythia suspensa* (Lianqiao)
MOL000422	Kaempferol	41.88	0.24	*Forsythia suspensa* (Lianqiao)
MOLO00522	Arctiin	34.45	0.84	*Forsythia suspensa* (Lianqiao)
MOL000006	Luteolin	36.16	0.25	*Forsythia suspensa* (Lianqiao)
MOL000791	Bicuculline	69.67	0.88	*Forsythia suspensa* (Lianqiao)
MOL000098	Quercetin	46.43	0.28	*Forsythia suspensa* (Lianqiao)
MOL004793	Nodakenetin	84.77	0.18	*Dendrobium nobile* (Shihu)
MOLO01999	Scoparone	74.75	0.09	*Dendrobium nobile* (Shihu)
MOLO05074	Shikimic acid	46.24	0.04	*Dendrobium nobile* (Shihu)

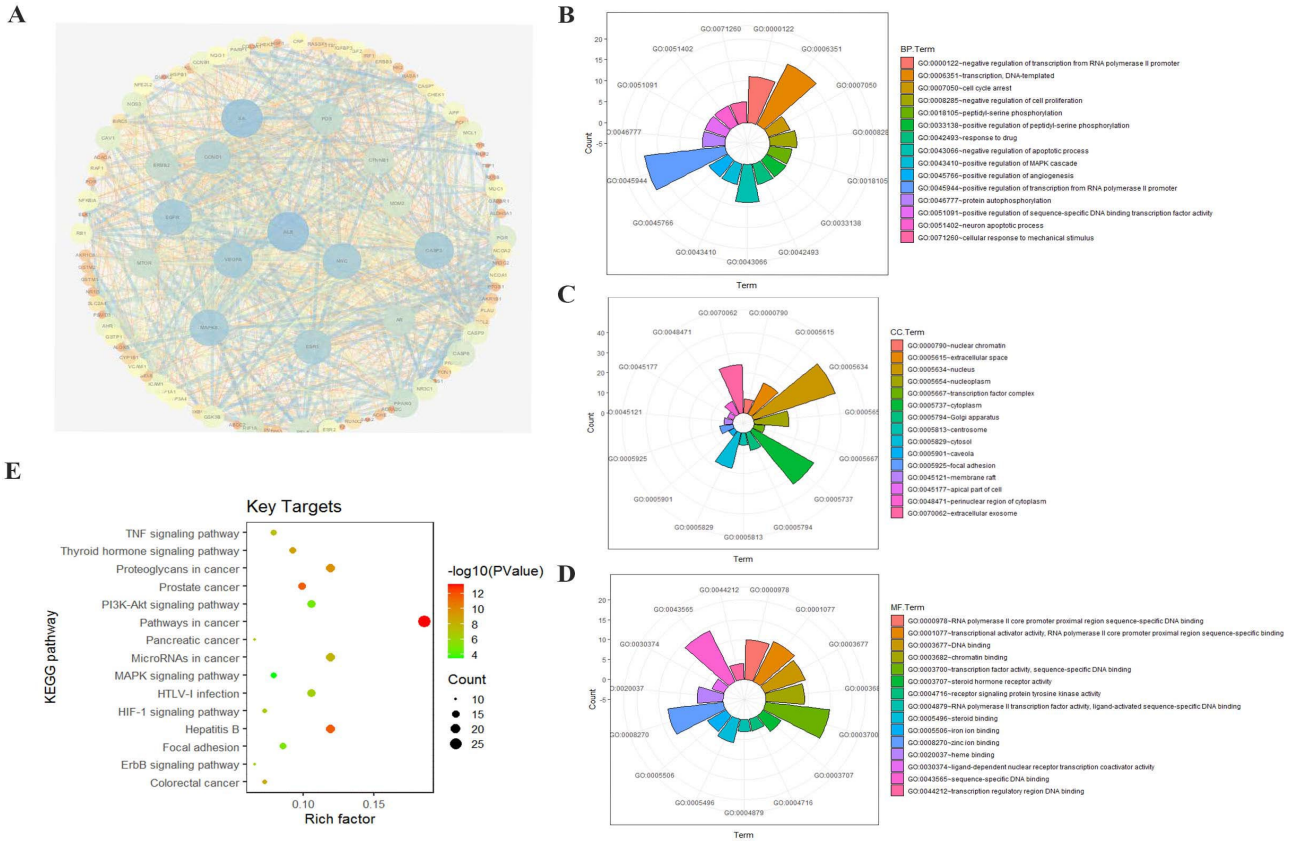

Figure A1. Construction of the Protein-Protein Interaction (PPI) network and functional enrichment analysis. (A) PPI network constructed via STRING and visualized in Cytoscape; larger nodes indicate higher degree. Core targets: ALB, IL6, CASP3, EGFR, VEGFA. (B) - (D) GO enrichment for Biological Process (BP), Cellular Component (CC), and Molecular Function (MF). (E) KEGG pathway enrichment highlighting PI3K-Akt, TNF, and MAPK signaling pathways.

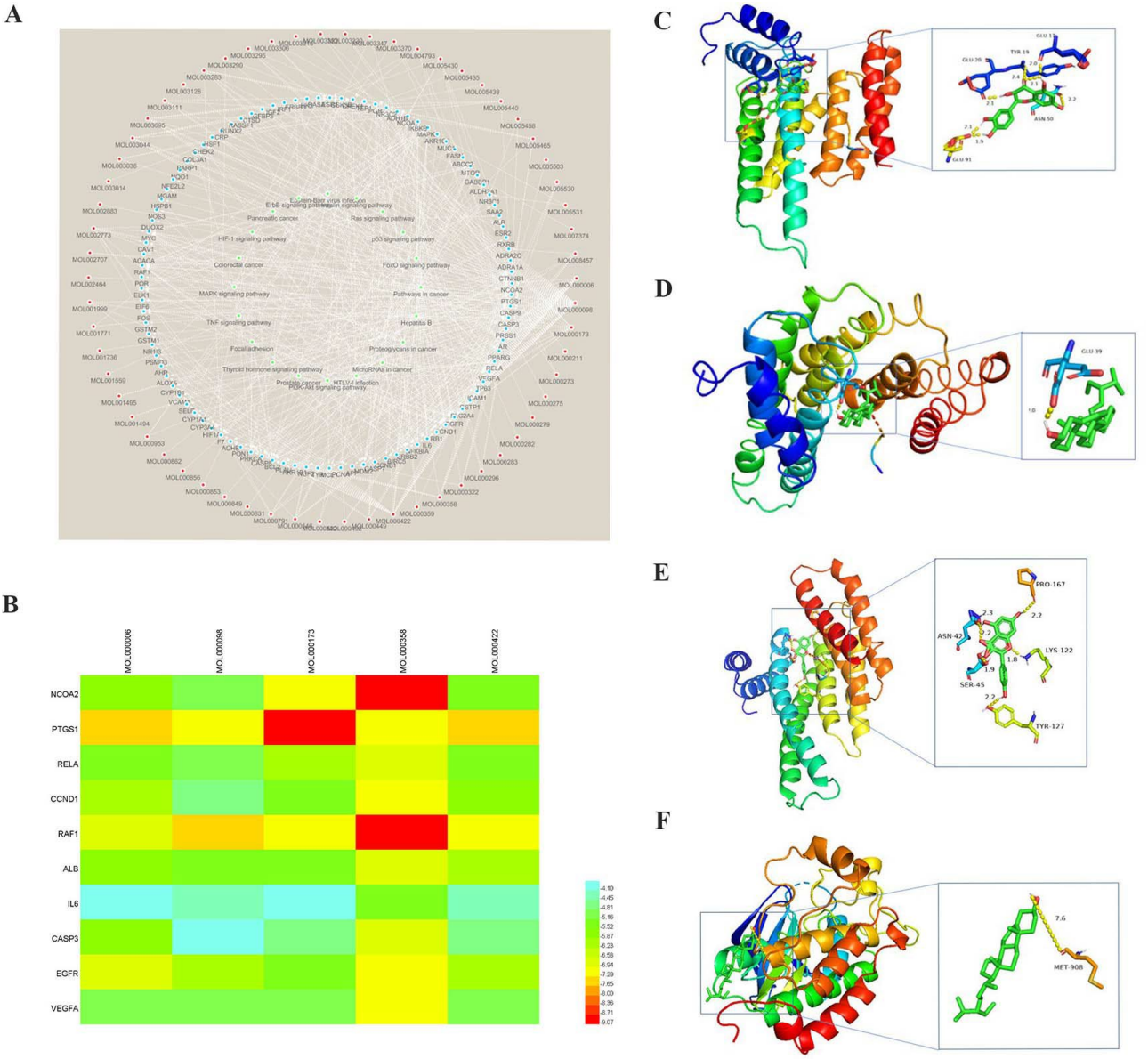

Figure A2. Construction and analysis of the "Active Compound-Key Target-Pathway" network and molecular docking results. (A) The "Active Compound-Key Target-Pathway" network included 62 active compounds, 101 target proteins, and 20 pathways. Red nodes represent active compounds, blue nodes represent key targets, and green nodes represent pathways. (B) Molecular docking binding energy heat map. (C) Docking of quercetin and RAF1. (D) Docking of beta-sitosterol and RAF1. (E) Docking of kaempferol and RAF1. (F) Docking of beta-sitosterol and EGFR.